



YjbH Requires Its Thioredoxin Active Motif for the Nitrosative Stress Response, Cell-to-Cell Spread, and Protein-Protein Interactions in *Listeria monocytogenes*

Brittany R. Ruhland,^a Michelle L. Reniere^a

^aUniversity of Washington, Department of Microbiology, Seattle, Washington, USA

ABSTRACT *Listeria monocytogenes* is a model facultative intracellular pathogen. Tight regulation of virulence proteins is essential for a successful infection, and the gene encoding the annotated thioredoxin YjbH was identified in two forward genetic screens as required for virulence factor production. Accordingly, an *L. monocytogenes* strain lacking *yjbH* is attenuated in a murine model of infection. However, the function of YjbH in *L. monocytogenes* has not been investigated. Here, we provide evidence that *L. monocytogenes* YjbH is involved in the nitrosative stress response, likely through its interaction with the redox-responsive transcriptional regulator SpxA1. YjbH physically interacted with SpxA1, and our data support a model in which YjbH is a protease adaptor that regulates SpxA1 protein abundance. Whole-cell proteomics identified eight additional proteins whose abundance was altered by YjbH, and we demonstrated that YjbH physically interacted with each in bacterial two-hybrid assays. Thioredoxin proteins canonically require active motif cysteines for function, but thioredoxin activity has not been tested for *L. monocytogenes* YjbH. We demonstrated that cysteine residues of the YjbH thioredoxin domain active motif are essential for *L. monocytogenes* sensitivity to nitrosative stress, cell-to-cell spread in a tissue culture model of infection, and several protein-protein interactions. Together, these results demonstrated that the function of YjbH in *L. monocytogenes* requires its thioredoxin active motif and that YjbH has a role in the posttranslational regulation of several proteins, including SpxA1.

IMPORTANCE The annotated thioredoxin YjbH in *Listeria monocytogenes* has been implicated in virulence, but its function in the cell is unknown. In other bacterial species, YjbH is a protease adaptor that mediates degradation of the transcriptional regulator Spx. Here, we investigated the function of *L. monocytogenes* YjbH and demonstrated its role in the nitrosative stress response and posttranslational regulation of several proteins with which YjbH physically interacts, including SpxA1. Furthermore, we demonstrated that the cysteine residues of the YjbH thioredoxin active motif are required for the nitrosative stress response, cell-to-cell spread, and some protein-protein interactions. YjbH is widely conserved among *Firmicutes*, and this work reveals its unique requirement of the thioredoxin-active motif in *L. monocytogenes*.

KEYWORDS ClpXP, bacterial two-hybrid, disulfide, nitrosative stress, posttranslational regulation, protease adaptor, protein-protein interactions, thioredoxins

Bacteria experience abrupt changes in their environment that require immediate adaptation. These perturbations and the ability to respond to them are often life or death situations, such as conditions of nutrient depletion or exposure to deadly reactive oxygen or nitrogen species. Changes at the transcriptional level can be enacted by transcriptional regulators, such as regulators that respond to oxidative stress (1).

Citation Ruhland BR, Reniere ML. 2020. YjbH requires its thioredoxin active motif for the nitrosative stress response, cell-to-cell spread, and protein-protein interactions in *Listeria monocytogenes*. *J Bacteriol* 202:e00099-20. <https://doi.org/10.1128/JB.00099-20>.

Editor Tina M. Henkin, Ohio State University

Copyright © 2020 Ruhland and Reniere. This is an open-access article distributed under the terms of the [Creative Commons Attribution 4.0 International license](https://creativecommons.org/licenses/by/4.0/).

Address correspondence to Michelle L. Reniere, reniere@uw.edu.

Received 21 February 2020

Accepted 28 March 2020

Accepted manuscript posted online 6 April 2020

Published 27 May 2020

Adaptation via protein regulation is rapid and can include posttranslational modifications to alter activity, regulated changes in protein solubility, and protease-dependent degradation (2–4).

Exquisite protein regulation is required for the Gram-positive, facultative intracellular pathogen *Listeria monocytogenes* to navigate the transition from environment to human host. To survive this transition, *L. monocytogenes* must properly respond to myriad oxidative and nitrosative stressors (5). After the host ingests *L. monocytogenes* from contaminated food or soil, the pathogen is either engulfed by phagocytic cells or taken up via receptor-mediated endocytosis (6). *L. monocytogenes* is able to survive the highly oxidative phagosome and escape into the reducing cytosol via the action of the pore-forming toxin listeriolysin O (LLO) (7). Once in the cytosol, *L. monocytogenes* begins replicating and recruits host actin via ActA, enabling cell-to-cell spread with actin-based motility (8, 9). Each stage of this intracellular life cycle requires tight regulation of virulence proteins. A forward genetic screen in *L. monocytogenes* for hypohemolytic mutants identified the annotated thioredoxin gene *yjbH* (*yjbH_{Lm}*) as being required for LLO secretion and virulence (10). A subsequent screen found *yjbH_{Lm}* is also required for ActA production, likely via posttranscriptional regulation of the actA 5' untranslated region (UTR) (11). Despite the importance of YjbH_{Lm} to virulence, its function in *L. monocytogenes* has not been explored.

YjbH is a cytosolic protein with an N-terminal thioredoxin domain and is conserved among *Firmicutes* (10, 12, 13). Much of what is known about YjbH comes from studies on *Bacillus subtilis*, in which it is a protease adaptor for the ArsC-family redox-responsive transcriptional regulator Spx (14). *B. subtilis* YjbH (YjbH_{Bs}) maintains low *B. subtilis* Spx (Spx_{Bs}) concentrations during steady state by binding to Spx_{Bs} and enhancing its ClpXP-mediated degradation (14–16). During disulfide stress, YjbH_{Bs} aggregation prevents binding to Spx_{Bs} and, therefore, results in increased Spx_{Bs} concentrations (17). Spx_{Bs} is then available to interact with the alpha C-terminal domain of the RNA polymerase to regulate gene expression (18–20). Spx_{Bs} upregulates over 100 genes, including redox-response genes, such as *trxA* and *trxB*, and represses over 170 genes (21, 22).

The interaction between YjbH_{Bs} and Spx_{Bs} has been demonstrated by coimmunoprecipitation and, more recently, the cocrystal structure of Spx_{Bs} with a thermostable YjbH homologue from *Geobacillus kaustophilus* (YjbH_{Gk}) (23, 24). YjbH_{Gk} is a multidomain protein containing a thioredoxin domain with an alpha-helical insertion and a C-terminal winged-helix domain connected by a linker region (24). Elements of the thioredoxin domain and the alpha-helical insertion are at the interface of the YjbH_{Gk}-Spx_{Bs} heterodimer (24). The physical interaction between YjbH_{Bs} and Spx_{Bs} is critical to the role of YjbH_{Bs} as a posttranslational regulator of Spx_{Bs} (16).

Although all YjbH homologues have a thioredoxin domain and many have the canonical cysteine-X-X-cysteine (CXXC) thioredoxin-active motif, thioredoxin activity has not been demonstrated. The active motif cysteines are essential for thioredoxins to reduce their substrates (25, 26). Both YjbH_{Lm} and YjbH_{Bs} have a CXXC motif in the thioredoxin domain, and the *Staphylococcus aureus* homologue (YjbH_{St}) has SXXC and CXC motifs (27). Cysteine residues are not required for YjbH-mediated degradation of Spx in either *B. subtilis* or *S. aureus* (27). The CXXC cysteines and the two cysteines located outside the CXXC motif in YjbH_{Lm} have never been tested for their contribution to YjbH function.

In this study, we aimed to elucidate the role of YjbH_{Lm}. *L. monocytogenes* encodes SpxA1, which is 83% identical in amino acid sequence to Spx_{Bs}. We showed that YjbH_{Lm} interacted with SpxA1 and was involved in the nitrosative stress response. Additionally, whole-cell mass spectrometry revealed 10 proteins with increased abundance in a $\Delta yjbH_{Lm}$ mutant. We found that YjbH_{Lm} physically interacted with nine of these proteins. Interestingly, our work demonstrated that YjbH_{Lm} uniquely requires its CXXC motif cysteine residues for function, unlike homologues in other species.

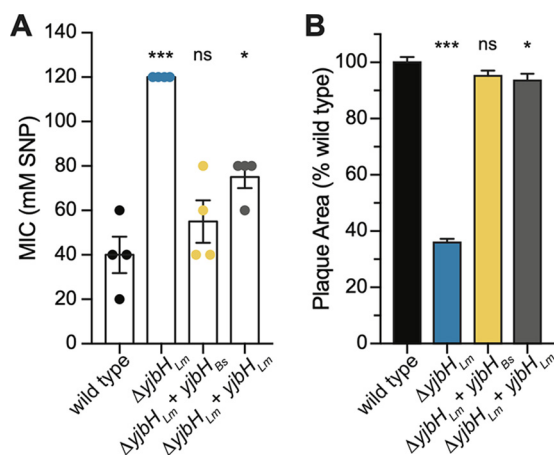


FIG 2 YjbH_{Bs} functionally complements $\Delta yjbH_{Lm}$ for SNP sensitivity and cell-to-cell spread. (A) Sensitivity to sodium nitroprusside (SNP) was measured by MIC determination in tryptic soy broth at 37°C. Data represent three biological replicates graphed as means and standard error of the mean (SEM). (B) Plaque area in murine L2 cells, normalized to wild-type *L. monocytogenes*. Data represent three biological replicates graphed as means and SEMs. In both panels, mutant strains are compared to the wild type by Student's unpaired *t* test (not significant [ns], $P > 0.05$; *, $P < 0.05$; ***, $P < 0.001$).

species, *yjbH_{Bs}* was expressed from the predicted *yjbH_{Lm}* native promoter at an ectopic locus in the *L. monocytogenes* $\Delta yjbH$ genome (28). Expression of *yjbH_{Bs}* complemented the $\Delta yjbH_{Lm}$ mutant (Fig. 2A), suggesting that despite the species' disparate phenotypes, essential functions of YjbH are conserved.

We next tested whether YjbH_{Bs} could functionally complement the $\Delta yjbH_{Lm}$ mutant during infection by using a plaque assay. Murine fibroblasts were infected, and cell-to-cell spread was measured 3 days postinfection (29). The $\Delta yjbH_{Lm}$ mutant formed plaques approximately 60% smaller than those formed by the wild type, indicating it is defective for cell-to-cell spread, as previously reported (11). The $\Delta yjbH_{Lm}$ strain expressing the *yjbH_{Bs}* allele formed plaques approximately the size of the wild type (Fig. 2B), demonstrating that YjbH_{Bs} is functional in *L. monocytogenes* during infection of mammalian cells.

***L. monocytogenes* YjbH and SpxA1 interact.** In other *Firmicutes*, the physical interaction between YjbH and Spx is critical for the bacteria to maintain redox homeostasis (15, 16, 24). Expression of *yjbH_{Bs}* in the $\Delta yjbH_{Lm}$ background restored its SNP sensitivity to wild-type levels, leading us to hypothesize that the interaction with the *L. monocytogenes* Spx homologue (SpxA1) may also be conserved. We attempted to perform a coimmunoprecipitation to test for interactions between YjbH_{Lm} and SpxA1. However, because both proteins are present in extremely low abundance in *L. monocytogenes* and YjbH proteins are prone to aggregation (15, 17), we were unable to detect an interaction. Instead, we used the bacterial adenylate cyclase two-hybrid (BACTH) system, in which proteins of interest are heterologously expressed in *Escherichia coli* BTH101 cells as fusion proteins with the *Bordetella pertussis* adenylate cyclase T18 and T25 domains (30, 31). BTH101 strains used in these assays harbor both T18 and T25 fusion protein plasmids, and if the proteins of interest interact, cAMP is produced, leading to β -galactosidase production.

BTH101 cells harboring YjbH_{Lm}-T18 and SpxA1-T25 expression plasmids grown overnight in rich broth demonstrated that YjbH_{Lm} and SpxA1 physically interact (Fig. 3). This interaction was specific, as no interaction was detected either between YjbH_{Lm} and the T25 domain alone or SpxA1 and the T18 domain alone. Because expressing the *yjbH_{Bs}* allele functionally complemented the $\Delta yjbH_{Lm}$ mutant, we next investigated interactions between the *L. monocytogenes* and *B. subtilis* proteins. We observed that YjbH_{Lm} interacted with Spx_{Bs}, and that YjbH_{Bs} interacted with SpxA1, confirming that this important physical interaction is conserved between *L. monocytogenes* and *B.*

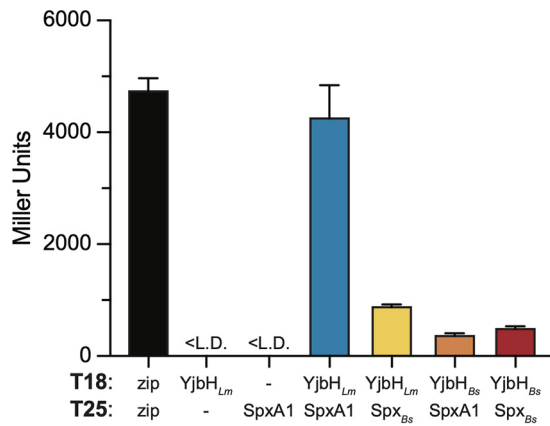


FIG 3 *L. monocytogenes* YjbH_{Lm} and SpxA1 physically interact. Interaction was measured by BACTH assay of overnight cultures of LB broth. The positive control is T18 and T25, with each fused to a leucine zipper region, and negative controls are YjbH_{Lm}-T18 with T25 alone and SpxA1-T25 with T18 alone. Data represent three biological replicates graphed as means and SEMs, with the exception of the SpxA1-T25 with T18 negative control, which represents two biological replicates.

subtilis proteins (Fig. 3). We also observed an interaction between YjbH_{Bs} and Spx_{Bs}, as previously reported (16, 23).

YjbH_{Lm} and SpxA1 are involved in the nitrosative stress response and LLO regulation. The only documented role for YjbH in *Firmicutes* is to modulate levels of Spx such that a strain lacking *yjbH* has increased Spx abundance (14, 16, 27). The physical interaction between YjbH_{Lm} and SpxA1 was conserved in *L. monocytogenes*, leading us to question if the phenotypes associated with the $\Delta yjbH_{Lm}$ strain are SpxA1 dependent. The roles of *yjbH_{Lm}* and *spxA1* were first examined in an SNP MIC assay. An *spxA1* knockdown strain (*P-spxA1::Tn* strain) that expresses 10-fold less *spxA1* transcript was used for these experiments, as a strain deleted for *spxA1* does not grow in the presence of oxygen (32). The *spxA1* knockdown strain grows aerobically and is more sensitive to hydrogen peroxide and diamide (11) but has not yet been tested in the presence of SNP. While the $\Delta yjbH_{Lm}$ mutant was 3-fold more resistant to SNP, the *P-spxA1::Tn* strain was much more sensitive to SNP than the wild type (Fig. 4A). If the $\Delta yjbH$ strain was more resistant to SNP due to increased SpxA1 abundance, as in other *Firmicutes*, then knocking down *spxA1* would restore $\Delta yjbH_{Lm}$ sensitivity to wild-type levels. Indeed, the MIC of the $\Delta yjbH_{Lm}$ *P-spxA1::Tn* strain was similar to that of the wild type (Fig. 4A). These data suggested that the increased resistance of the $\Delta yjbH_{Lm}$ strain to SNP was due to increased SpxA1 abundance.

In addition to its role in the nitrosative stress response, *yjbH_{Lm}* is required for LLO production and/or secretion (10, 11). The virulence factor LLO is essential for *L. monocytogenes* to escape the phagosome during infection and is also expressed at low levels during growth in rich broth. We examined whether the $\Delta yjbH_{Lm}$ defect in LLO secretion is SpxA1 dependent by analyzing immunoblots of secreted proteins in broth. As previously published (11), both the $\Delta yjbH_{Lm}$ and *P-spxA1::Tn* mutants secreted less LLO than the wild type *in vitro* (Fig. 4B). LLO secretion in the double mutant was not significantly different from the *spxA1* knockdown strain, suggesting that the LLO secretion defect of the $\Delta yjbH_{Lm}$ strain is not solely SpxA1 dependent (Fig. 4C). We hypothesized that the LLO defect in the $\Delta yjbH_{Lm}$ strain happens at the level of translation or secretion. Indeed, hly transcript abundance was unchanged from that of the wild type (1.1-fold change in the $\Delta yjbH_{Lm}$ strain compared to the wild type, $P = 0.76$). The observation that the YjbH_{Lm}-dependent posttranslational regulation of LLO may not entirely be explained by SpxA1 levels led us to speculate that YjbH_{Lm} may interact with additional proteins in *L. monocytogenes*.

Whole-cell proteomic profiling of *L. monocytogenes* $\Delta yjbH$. Given the known role of YjbH_{Bs} as a protease adaptor, we sought to determine whether YjbH_{Lm} is involved in

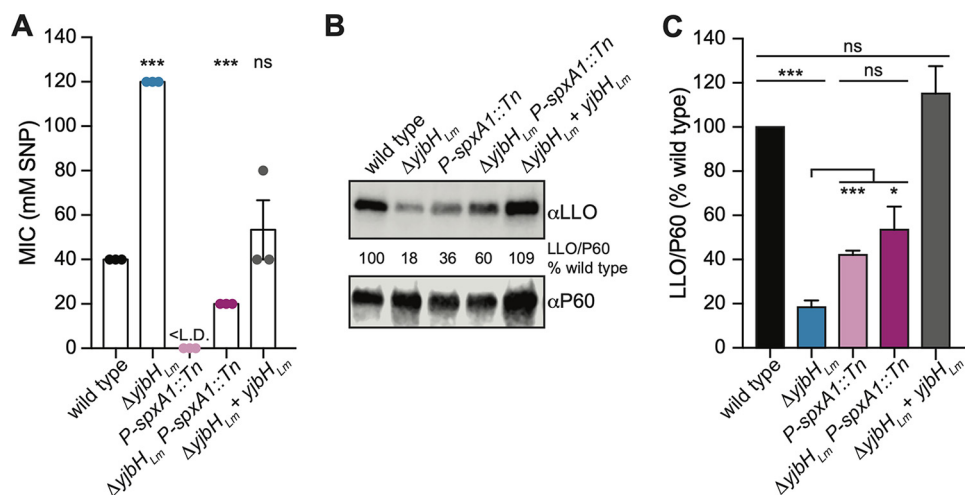


FIG 4 YjbH_{Lm} and SpxA1 are involved in the nitrosative stress response and LLO regulation. (A) Sensitivity to SNP was measured by MIC in tryptic soy broth at 37°C. The P-spxA1::Tn strain transcribes 10-fold less *spxA1* than the wild type and grows aerobically (11). Data represent three biological replicates graphed as means and SEMs. <L.D. indicates the MIC was below the limit of detection. All mutant strains are compared to the wild type by Student's unpaired *t* test (ns, *P* > 0.05; ****, *P* < 0.0001). (B) One representative immunoblot of LLO secretion measured in cultures grown in BHI broth at 37°C. The protein P60 was used as a loading control. Immunoblots were analyzed by calculating the ratio of LLO/P60 as a percentage of the wild type. (C) Quantification of three biological replicates of LLO secretion shown in panel B, graphed as means and SEMs. All statistical analyses are Student's unpaired *t*-tests (ns, *P* > 0.05; *, *P* < 0.05; ***, *P* < 0.001).

the regulation of proteins other than SpxA1 in *L. monocytogenes*. YjbH_{Lm} abundance was first investigated under various growth conditions to identify ideal parameters for this analysis. In *B. subtilis*, the abundance of soluble YjbH_{Bs} is affected by stressors, such as ethanol, diamide, and heat (17). However, native YjbH_{Lm} was undetectable under all conditions tested, including elevated temperature and treatment with sublethal concentrations of ethanol, diamide, SNP, or hydrogen peroxide (see Fig. S1 in the supplemental material). Therefore, early stationary phase was selected for proteomic analysis due to the pronounced LLO phenotype exhibited by the $\Delta yjbH_{Lm}$ strain in rich broth at this time point (Fig. 4B and C), indicating that YjbH_{Lm} is likely functional under this growth condition. Whole-cell proteomic profiling was used as an unbiased approach to identify proteins with altered abundance in the $\Delta yjbH_{Lm}$ strain. Cultures were prepared in biological triplicate, and proteins were analyzed by liquid chromatography-tandem mass spectrometry (LC-MS/MS). The fold change of average peptide spectral counts was calculated between wild-type and $\Delta yjbH_{Lm}$ samples and analyzed with Student's *t* test (see Data Set S1 in the supplemental material).

We focused on the nine proteins significantly more abundant in the $\Delta yjbH_{Lm}$ strain than the wild type (Table 1). SpxA1 was also more abundant in the $\Delta yjbH_{Lm}$ strain, although this change was not statistically significant due to its complete absence in wild-type samples and the variability of peptide counts between $\Delta yjbH_{Lm}$ replicates. These data demonstrated for the first time that SpxA1_{Lm} is more abundant in the absence of yjbH_{Lm}, supporting the hypothesis that YjbH_{Lm} functions similarly to YjbH_{Bs} with respect to regulating SpxA1 abundance (14, 16). To assess whether the observed changes in protein concentration were the result of transcriptional or posttranscriptional regulation, quantitative reverse transcriptase PCR (RT-PCR) was performed comparing gene expression in wild-type and $\Delta yjbH_{Lm}$ cultures (Fig. 5A). Five transcripts (*lmo1258*, *lmo1387*, *lmo1636*, *lmo1782*, and *lmo2390*) were significantly more abundant in the $\Delta yjbH_{Lm}$ strain than in the wild type, suggesting that increased protein concentration may result from transcriptional regulation. It is possible that these five genes are also posttranscriptionally regulated to result in increased protein levels. Five genes (*spxA1*, *lmo0218*, *lmo0256*, *lmo0597*, and *lmo1647*) were expressed at or below wild-type levels in the $\Delta yjbH_{Lm}$ strain, indicating that the increases in protein abundance

TABLE 1 Whole-cell proteomics revealed proteins more abundant in the $\Delta yjbH_{Lm}$ strain than in the wild type

Gene locus	Predicted function	Protein	Avg spectral peptide count ^a of:		P value
			Wild type	$\Delta yjbH_{Lm}$ strain	
<i>Imo0218</i>	Polyribonucleotide nucleotidyltransferase domain		1.53	3.68	0.006
<i>Imo0256</i>	S-Adenosylmethionine-dependent methyltransferase activity		1.22	3.00	0.045
<i>Imo0597</i>	Crp/Fnr-family transcriptional regulator		0.31	2.24	0.006
<i>Imo1258</i>	Putative lipase		ND	2.82	0.028
<i>Imo1387</i>	Pyroline-5-carboxylate reductase		0.61	2.68	0.045
<i>Imo1636</i>	ABC transporter ATP-binding protein		2.14	4.47	0.011
<i>Imo1647</i>	1-Acylglycerol-3-phosphate O-acyltransferase		0.61	2.56	0.007
<i>Imo1782</i>	3'-Exo-deoxyribonuclease		1.23	3.93	0.009
<i>Imo2191</i>	Transcriptional regulator	SpxA1	ND	2.76	0.214
<i>Imo2390</i>	Ferredoxin-NADP reductase 2		2.45	5.94	0.005

^aData are from three independent samples. ND, no peptides were detected.

observed by mass spectrometry were not due to transcriptional regulation. These results suggested that YjbH_{Lm} is involved in the posttranscriptional or posttranslational regulation of multiple proteins in *L. monocytogenes*.

YjbH interacts with multiple *L. monocytogenes* proteins. BACTH assays were next used to test the hypothesis that YjbH_{Lm} function in *L. monocytogenes* involves direct interaction with proteins in addition to SpxA1. BTH101 strains were generated that each harbored a plasmid expressing YjbH_{Lm}-T18 in addition to a plasmid expressing a T25 fusion with each of the proteins listed in Table 1. We were unable to express *Imo0597* in *E. coli* and, therefore, could not test for an interaction with YjbH_{Lm}. Interestingly,

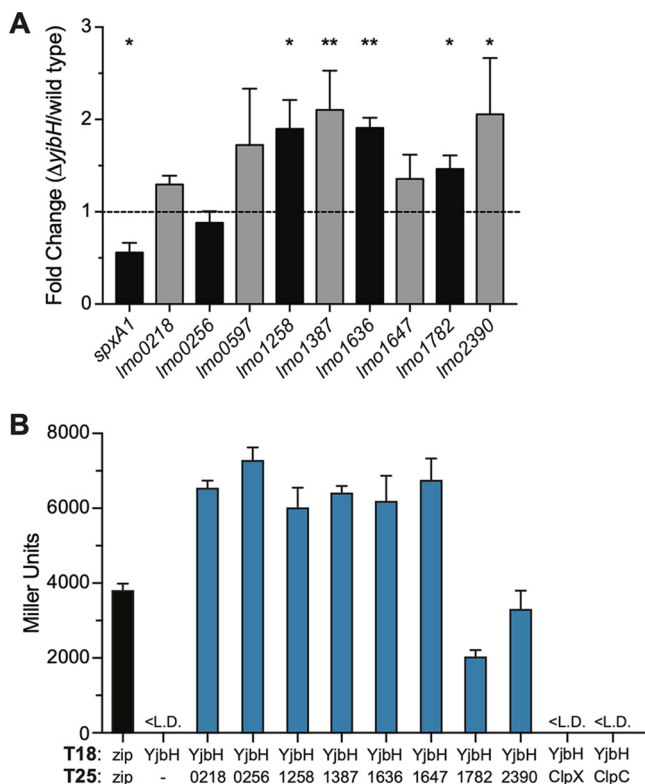


FIG 5 YjbH_{Lm} interacts with multiple *L. monocytogenes* proteins. (A) Gene expression was measured in wild-type and $\Delta yjbH_{Lm}$ strains by quantitative RT-PCR and is graphed as the fold change in the $\Delta yjbH_{Lm}$ strain compared to wild type. Student's unpaired *t* test was used to compare transcript fold changes between the $\Delta yjbH_{Lm}$ strain and wild type (*, *P* < 0.05; **, *P* < 0.01). (B) Interactions with YjbH_{Lm} were measured by BACTH assay of overnight cultures of LB broth. T25 fusion proteins are labeled with their *Imo* locus number or protein name. Data represent three biological replicates graphed as means and SEMs. <L.D. indicates Miller units below the limit of detection.

BACTH assays revealed a physical interaction between YjbH_{Lm} and each of the eight proteins identified by mass spectrometry as more abundant in the $\Delta yjbH_{Lm}$ strain (Fig. 5B). Some chaperone proteins are known to interact with the ATPase and substrate-binding subunit of the protease as well as with the protein substrate (33). ClpC and ClpX ATPase subunits have both been implicated in Spx_{Bs} degradation in *B. subtilis*, although YjbH_{Bs}-mediated Spx_{Bs} degradation is specific to ClpXP (16, 34). However, we were unable to detect an interaction between YjbH_{Lm} and ClpC or ClpX by BACTH (Fig. 5B). Together, these results indicated that YjbH_{Lm} is able to physically interact with at least nine *L. monocytogenes* proteins, including SpxA1.

YjbH cysteine residues influence function and protein-protein interactions.

Although all YjbH homologues have a thioredoxin-like domain and many have a CXXC catalytic motif (Fig. 1A), it remains unknown whether thioredoxin activity is important for YjbH function in *L. monocytogenes*. Canonical thioredoxin activity involves a transient intermolecular disulfide bond between the thioredoxin CXXC motif and substrate proteins. To test the role of the four cysteine residues of YjbH_{Lm}, $\Delta yjbH_{Lm}$ strains were engineered to express *yjbH_{Lm}* encoding cysteine-to-alanine point mutations from the predicted *yjbH_{Lm}* native promoter (see Table S1 in the supplemental material). These strains include each of the four cysteines mutated individually (YjbH^{C27A}, YjbH^{C30A}, YjbH^{C63A}, and YjbH^{C89A}), as well as a mutated CXXC motif (YjbH^{C27/30A}), both cysteines outside the CXXC motif mutated (YjbH^{C63/89A}), and all four cysteine residues mutated (YjbH^{Δcys}). The mutant YjbH_{Lm} proteins were as abundant as wild-type YjbH_{Lm} when overexpressed (see Fig. S2 in the supplemental material), indicating that the cysteine-to-alanine substitutions did not affect overall protein stability.

To investigate the role of the cysteine residues in YjbH_{Lm} function, the aforementioned mutants were tested for cell-to-cell spread by plaque assay, nitrosative stress resistance via SNP MIC assay, and LLO secretion by immunoblot. The data revealed that YjbH^{C63A}, YjbH^{C89A}, and YjbH^{C63/89A} fully complemented the $\Delta yjbH_{Lm}$ mutant for cell-to-cell spread (Fig. 6A, dark purple bars), SNP resistance (Fig. 6B), and LLO secretion (Fig. 6C and D). However, all strains with mutations in the CXXC motif failed to fully rescue the $\Delta yjbH_{Lm}$ phenotypes (Fig. 6A to D, lavender bars). These data suggested that the CXXC motif is required for YjbH_{Lm} function in the context of the known phenotypes, while the other two cysteine residues are dispensable.

We next used BACTH assays to assess whether the YjbH_{Lm} cysteine residues are required for protein-protein interactions. YjbH^{C63/89A} retained interactions with all tested proteins except SpxA1 and Lmo0218 (Fig. 6E). The protein with an altered CXXC motif (YjbH^{C27/30A}) interacted only with Lmo1258 and Lmo1387 (Fig. 6E). Together, these results demonstrated that YjbH_{Lm} cysteine residues are required for its physical interaction with some proteins.

As described previously, the CXXC motifs of thioredoxin domains are known to form transient intermolecular disulfide bonds with substrate proteins. Of those tested here, only the following proteins contain cysteine residues: SpxA1, Lmo0256, Lmo1258, Lmo1387, Lmo1782, and Lmo2390 (Fig. 6E, underlined). If intermolecular disulfide bonds involving the CXXC motif were essential for YjbH_{Lm} to interact with any of the cysteine-containing proteins, we would expect the interacting proteins to bind the wild-type YjbH_{Lm} protein but not the YjbH^{C27/30A} mutant. The observation that YjbH^{C27/30A} could still bind two proteins suggested that YjbH_{Lm} can interact with proteins at a site other than the CXXC motif. These results demonstrated that not all YjbH_{Lm} protein interactions require intermolecular disulfide bond formation, as is typical for thioredoxins. However, we cannot rule out a role for disulfide bonds in all interactions.

DISCUSSION

In this study, we investigated the role of the annotated thioredoxin YjbH_{Lm} in *L. monocytogenes*. Strains lacking *yjbH_{Lm}* do not have a growth defect intracellularly or in rich broth but exhibit defects in cell-to-cell spread, the production of ActA and LLO, and are attenuated in a mouse model of infection (11). Our results demonstrated that YjbH_{Lm} physically interacts with the redox-responsive transcriptional regulator SpxA1

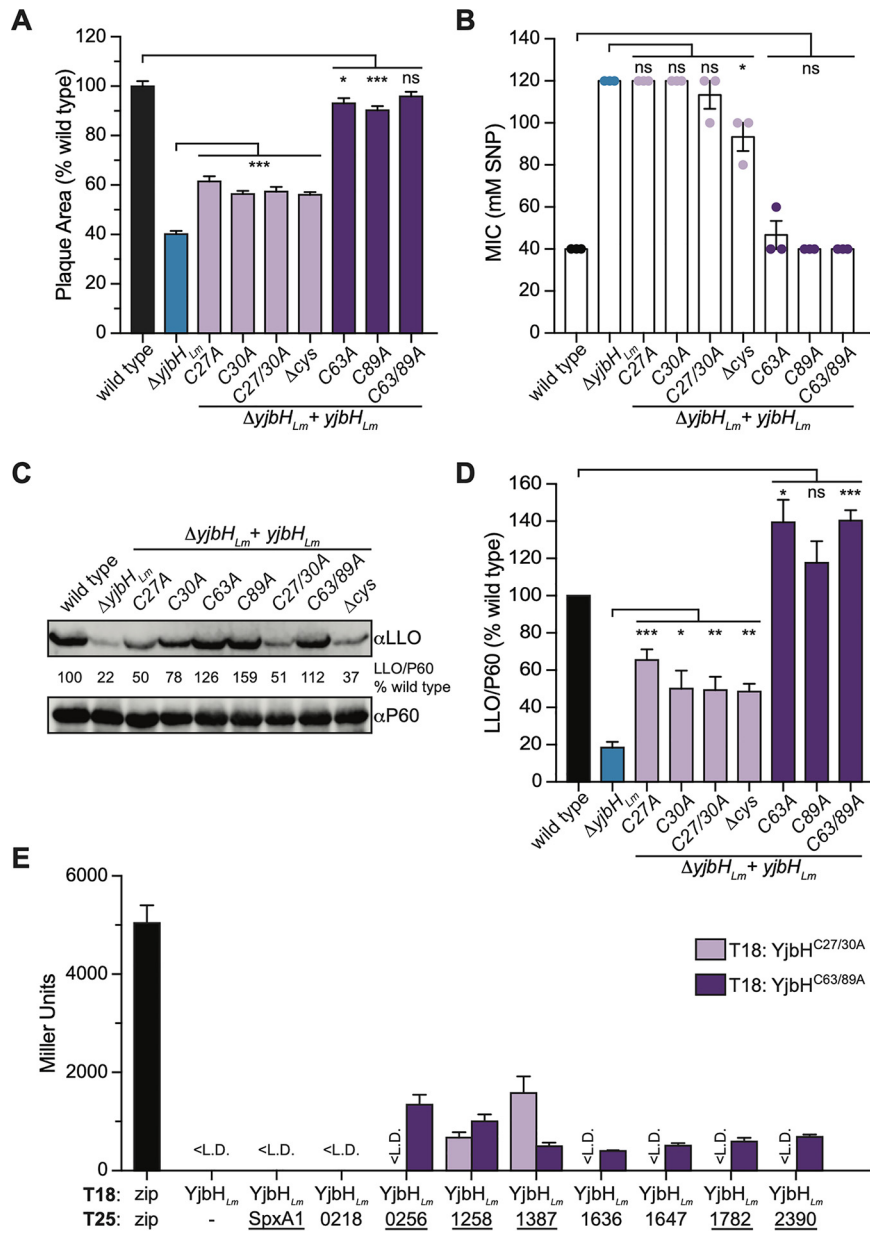


FIG 6 Cysteine residues contribute to YjbH_{Lm} function. (A) Plaque area in murine L2 cells, normalized to wild-type *L. monocytogenes*. Data represent three biological replicates graphed as means and SEMs. (B) Sensitivity to SNP was measured by MIC determination in tryptic soy broth at 37°C. Data represent three biological replicates graphed as means and SEMs. (C) One representative immunoblot of LLO secretion, measured as in Fig. 4C. (D) Graphed data represent three biological replicates of LLO secretion shown in panel C, graphed as means and SEMs. (E) Interactions with YjbH^{C27/30A} and YjbH^{C63/89A} were determined by BACTH assay as in Fig. 5B. Gene names that are underlined encode proteins with at least one cysteine residue. <L.D. indicates Miller units below the limit of detection. Data represent three biological replicates graphed as means and SEMs. In panels A, B, and D, Student's *t* test was used to compare lavender bar data to data for the $\Delta yjbH_{Lm}$ strain and dark purple bar data to data for the wild type (ns, *P* > 0.05; *, *P* < 0.05; **, *P* < 0.01; ***, *P* < 0.001).

and that the $\Delta yjbH_{Lm}$ strain is more resistant to nitrosative stress than the wild type in an SpxA1-dependent manner. This study also presented data that suggest a possible SpxA1-independent role for YjbH_{Lm} in LLO secretion. Whole-cell proteomics provided a more holistic picture of the scope of YjbH_{Lm} function, revealing several proteins whose abundance was YjbH_{Lm} dependent. Furthermore, eight proteins that were more abundant in the $\Delta yjbH_{Lm}$ strain physically interacted with YjbH_{Lm} in BACTH assays. The

interactions of YjbH_{Lm} with SpxA1 and six other proteins were disrupted in the absence of an intact YjbH_{Lm} CXXC motif. Results from this study demonstrated that YjbH_{Lm} requires its thioredoxin active motif for SNP sensitivity, cell-to-cell spread, and LLO secretion and that YjbH_{Lm} plays a role in the posttranslational regulation of several proteins.

In *B. subtilis*, YjbH_{Bs} physically interacts with Spx_{Bs} to accelerate degradation of Spx_{Bs} by the ClpXP protease. The results presented here suggest that YjbH_{Lm} functions similarly as a protease adaptor for SpxA1. First, BACTH assays demonstrated a physical interaction between YjbH_{Lm} and SpxA1. YjbH_{Lm} did not interact with the protease substrate-binding subunits ClpC or ClpX, although this was consistent with YjbH_{Bs}, which does not physically interact with ClpX (15). Instead, YjbH_{Bs} acts as an adaptor by lowering the conformational entropy of Spx_{Bs}, thereby increasing the efficiency of Spx_{Bs} binding to ClpX (24). We predict this mechanism is conserved in *L. monocytogenes*, as SpxA1 shares 83% amino acid identity with Spx_{Bs} and expressing *spx_{Bs}* functionally complements the Δ *spxA1* mutant (32). The second piece of evidence that YjbH_{Lm} is a protease adaptor for SpxA1 comes from whole-cell proteomics, which revealed increased SpxA1 protein levels in the Δ *yjbH_{Lm}* strain. Although protein levels were increased, *spxA1* transcript abundance was decreased in the Δ *yjbH_{Lm}* strain, indicating YjbH_{Lm}-dependent posttranscriptional regulation. Finally, the Δ *yjbH_{Lm}* strain with increased SpxA1 abundance had a corresponding increase in SNP resistance, demonstrating that the response to nitrosative stress in *L. monocytogenes* is SpxA1 dependent. Taken together, these results support a model in which YjbH_{Lm} is a protease adaptor that regulates SpxA1 protein abundance in *L. monocytogenes*.

It is interesting to note that the *L. monocytogenes* Δ *yjbH* mutant was more resistant to nitrosative stress, while the *B. subtilis* and *S. aureus* Δ *yjbH* mutants are more sensitive (12, 35). However, expressing the YjbH_{Bs} protein in the Δ *yjbH_{Lm}* strain fully restored its sensitivity to SNP. While these results may seem counterintuitive at first, we propose that the nitrosative stress phenotypes of bacteria lacking *yjbH* are dependent on factors regulated by Spx. We demonstrated that both YjbH_{Lm} and YjbH_{Bs} interact with SpxA1 and will, therefore, similarly affect the expression of SpxA1-dependent proteins. Defining the *L. monocytogenes* SpxA1 regulon is the next step to more completely define the differences between the organisms with respect to the differing YjbH-dependent responses to nitrosative stress.

Regulation of LLO production, secretion, and activity is complex and incompletely understood in *L. monocytogenes* (36, 37). YjbH_{Lm} was found to play a role in LLO regulation over a decade ago; yet, the mechanism behind this phenotype remains to be elucidated. We demonstrated here that the Δ *yjbH_{Lm}* defect in LLO secretion is likely partially SpxA1 independent. The Δ *yjbH_{Lm}* strain, which has more SpxA1 than the wild type, is severely deficient in LLO secretion. Conversely, the *spxA1* knockdown strain is also deficient in LLO. Together, these data revealed that LLO production is partially regulated in an SpxA1-dependent manner. Although SpxA1 is a transcriptional regulator and the *hly* transcript is unchanged, this regulation could be through posttranscriptional effects of the SpxA1 regulon. However, the fact that deleting *yjbH_{Lm}* in the *spxA1* knockdown strain did not rescue the LLO secretion defect suggests that part of this phenotype may be YjbH_{Lm} dependent and SpxA1 independent. No other studies on a YjbH homologue have presented evidence of Spx-independent functions of YjbH.

To elucidate YjbH_{Lm} function in an unbiased manner, we performed whole-cell proteomics on the Δ *yjbH_{Lm}* strain. In this study, we focused on proteins that were more abundant in the absence of *yjbH_{Lm}*, due to the known role of YjbH_{Bs} as a protease adaptor. With the exception of SpxA1, we concentrated on proteins whose increased abundance was statistically significant. It is possible that more proteins on this list are biologically significant but fall outside the bounds of statistical significance. There was also an extensive list of proteins significantly less abundant in the Δ *yjbH_{Lm}* strain than the wild type (see Table S2 in the supplemental material). While the study of these proteins was outside the scope of this work, future work will investigate how YjbH_{Lm} is capable of increasing the concentration of proteins like LLO when its only known role

is that of a protease adaptor. Even more intriguing is the fact that YjbH_{Lm} regulates two transcription factors, namely SpxA1 and Lmo0597. The regulons of SpxA1 and Lmo0597 have not been reported, and thus, it is unknown how altering levels of SpxA1 and Lmo0597 may contribute to $\Delta yjbH_{Lm}$ phenotypes. Of the five genes significantly increased in expression in the $\Delta yjbH_{Lm}$ strain, only one has a homologue in *B. subtilis* that is regulated by Spx_{Bs}. The putative 3'-exo-DNase *lmo1782* is 69% identical to *exoA* and upregulated by Spx_{Bs} during diamide stress (21). Ongoing experiments are aimed at deciphering the downstream effects of YjbH-dependent regulation of SpxA1 and Lmo0597.

Protease adaptor activity is dependent on direct interactions between the adaptor and substrate proteins. In BACTH assays with *L. monocytogenes* proteins, we found that YjbH_{Lm} interacted with 8 out of 10 tested proteins in addition to SpxA1. This finding was intriguing, as the only characterized YjbH_{Bs} interacting partners are Spx_{Bs} and the small inhibitor protein YirB, which is not conserved among *Firmicutes* and is not present in *L. monocytogenes*. An unbiased yeast two-hybrid screen of a *B. subtilis* genomic fusion library detected seven additional proteins that interacted with YjbH_{Bs} (23). Thus, while there is precedent for YjbH_{Bs} to bind proteins other than Spx_{Bs}, it is not known if any of these uncharacterized binding partners contribute to YjbH_{Bs} function. In *L. monocytogenes*, whole-cell proteomics showed that SpxA1 and the eight uncharacterized interacting partners were more abundant in the $\Delta yjbH_{Lm}$ strain, raising the possibility that YjbH_{Lm} posttranslationally regulates other proteins in addition to SpxA1. From their predicted functions, it was not obvious what these interacting partners have in common or what roles they may play in the cell. However, the ability of YjbH_{Lm} to interact with such a wide variety of proteins will inform future work to explain the myriad phenotypes exhibited by *L. monocytogenes* $\Delta yjbH_{Lm}$.

YjbH homologues share a conserved thioredoxin domain at the N terminus. A CXXC motif is required for catalytic activity in thioredoxin family proteins, but YjbH_{Bs} and YjbH_{sa} do not require CXXC motif cysteines for function (17, 27). We demonstrated here that the cysteine residues of the YjbH_{Lm} CXXC motif were required to fully complement a $\Delta yjbH_{Lm}$ mutant for SNP sensitivity, LLO secretion, and cell-to-cell spread. However, the YjbH_{Lm} protein with a mutated CXXC motif still retained partial functionality, perhaps through protein-protein interactions at a site other than the CXXC motif. For example, two out of nine proteins (Lmo1258 and Lmo1387) were still able to interact with YjbH^{C27/30A}, which lacks a functional CXXC motif. The two cysteine residues located outside the CXXC motif were required for interacting with SpxA1 and Lmo0218, although C63 and C89 were dispensable for YjbH function during cell-to-cell spread and SNP stress. In *B. subtilis*, the YjbH_{Bs} cysteine residues are not required for enhancing Spx_{Bs} degradation or for autoaggregation (17, 27). Cysteines are also dispensable to YjbH_{sa} function in virulence and Spx_{sa} degradation (27, 35). YjbH_{sa} does not contain a CXXC motif but instead has an SXXC motif that aligns with the *L. monocytogenes* and *B. subtilis* N-terminal CXXC motif and a CXC motif at nucleotide position 114 to 116 (27, 35). The lack of conservation of the CXXC motif across all YjbH homologues and the apparent lack of conserved cysteine essentiality suggest either that thioredoxin activity is not necessary for function or that CXXC motifs have disparate functions between species.

This is the first work to characterize YjbH_{Lm} and will serve as a foundation for future studies aimed at uncovering the full scope of its role. YjbH_{sa} transcomplements $\Delta yjbH_{Bs}$ (27), and we have shown here that YjbH_{Bs} complements the *L. monocytogenes* mutant. Together with our findings that $\Delta yjbH_{Lm}$ results in increased SpxA1 abundance, which indicates that YjbH_{Lm} is posttranslationally regulating SpxA1, this demonstrates conserved function between *Firmicutes*. However, YjbH_{Lm} has unique characteristics that set it apart from other homologues. For example, YjbH_{Lm} is present in very low abundance under every growth condition examined, the LLO secretion defect is at least partially SpxA1 independent, YjbH_{Lm} has a role in the posttranscriptional regulation of at least nine proteins, and YjbH_{Lm} requires the CXXC motif cysteines for function. The basic characterization presented here is, thus, both broadly applicable to other *Firmi-*

cutes species and a step forward in understanding the uniquely complex role of Yj**b**_{Lm} in *L. monocytogenes*.

MATERIALS AND METHODS

Bacterial strains and culture conditions. All *L. monocytogenes* strains are a derivative of strain 10403S (38, 39). *L. monocytogenes* strains were cultivated in brain heart infusion broth (BHI; Difco) or tryptic soy broth (TSB; Difco) shaking at 37°C, and *E. coli* strains were cultivated in LB broth (Miller) shaking at 37°C. Antibiotics were used at the following concentrations for Gram-negative strains: 100 µg/ml (carbenicillin) and 50 µg/ml (kanamycin). Antibiotics were used at the following concentrations for Gram-positive strains: 200 µg/ml (streptomycin), 5 µg/ml (chloramphenicol), and 2 µg/ml (tetracycline).

Cloning and plasmid construction. The integrating plasmid pPL2 was used to generate *L. monocytogenes* mutants, as previously described (40). Briefly, genes of interest were amplified from *L. monocytogenes* 10403S and digested with the same restriction endonucleases (New England BioLabs) used to digest the pPL2 vector, followed by a ligation reaction to join the insert with the vector. Ligation products were transformed into *E. coli* SM10 and sequenced before proceeding.

Constructed plasmids in *E. coli* SM10 were transconjugated into recipient *L. monocytogenes* strains by mixing donor and recipient cells 1:1 and incubating on BHI agar plates for 4 to 24 h at 30°C. Cell mixtures were then streaked onto BHI plates containing streptomycin and chloramphenicol to select for cells containing the pPL2 plasmid. Resulting colonies were restreaked for isolation and sequenced before use.

The $\Delta yj**b**H P-spxA1::Tn$ strain was constructed by transducing the *himar1* transposon into the $\Delta yj**b**H$ background, as previously described (10, 41).

Plasmids for the BACTH assays were constructed via Gibson assembly using the NEBuilder HiFi DNA assembly master mix (New England BioLabs). Briefly, genes of interest were amplified with 5' (ATGGG GTCCAGCGGCTGGATCC) and 3' (GCTGCAGGAGGCAAGTGGAGCGAGC) linker regions identical to linker regions flanking a *ccdB* toxin cassette in the pUT18x, pUT18Cx, pKT25x, and pKNT25x vectors, which were generously gifted to us by Aaron Whiteley (42). Vectors were linearized with BamHI and PstI endonucleases that excised the *ccdB* cassette and then were combined in the NEB master mix with an insert encoding the gene of interest, as directed by the manufacturer. The reaction mix was transformed into *E. coli* XL1-Blue cells. XL1-Blue cells containing single BACTH vectors were sequenced, and their plasmid DNA was harvested. Each BTH101 strain used in BACTH assays was cotransformed with one T18 plasmid and one T25 plasmid. After cotransformations, all BTH101 strains were cultivated in both kanamycin and carbenicillin at all times to retain both plasmids.

MIC assays. *L. monocytogenes* cultures were grown overnight in TSB medium containing streptomycin at 37°C. Assays were performed in 96-well plates. Each well contained 200 µl total of TSB medium, SNP (solution made fresh daily in TSB with streptomycin), and 2×10^4 CFU. Each *L. monocytogenes* strain was tested in 120 mM, 100 mM, 80 mM, 60 mM, 40 mM, 20 mM, 10 mM, and 0 mM SNP. Overnight cultures were diluted in phosphate-buffered saline (PBS) to 10^4 CFU/ml before being added to assay wells. Plates were incubated in shaking plate incubator at 37°C for 24 h, and then the MIC for each strain was determined as the lowest concentration of SNP with no visible bacterial growth.

L2 plaque assays. Plaque assays were performed according to published protocols (29). Briefly, L2 fibroblasts were seeded at a density of 1.2×10^6 per well in a 6-well dish, and overnight cultures of *L. monocytogenes* were incubated at 30°C in BHI broth. The next day, cultures were diluted 1:10 in sterile PBS and 5 µl was used to infect cells for 1 h before being washed twice with sterile PBS. Agarose overlays containing Dulbecco's modified Eagle's medium (DMEM) and gentamicin were added to the wells, and plates were incubated for 2 days before the cells were stained with neutral red dye. Plaques were imaged 24 h later, and plaque areas were determined using Image J software (43). All plaque data represent three biological replicates.

Immunoblotting for the LLO protein. Overnight *L. monocytogenes* cultures were subcultured 1:10 into BHI medium containing streptomycin and were incubated for 5 h at 37°C with shaking. Cultures were pelleted, and the supernatant was then trichloroacetic acid (TCA)-precipitated to collect protein, boiled in loading dye, and separated by gel electrophoresis. Proteins were then transferred to a polyvinylidene difluoride (PVDF) membrane (Bio-Rad), and the membrane was blocked with Odyssey blocking buffer (Li-Cor Biosciences). Proteins of interest were detected using polyclonal rabbit anti-LLO antibody (from the Portnoy Laboratory, University of California at Berkeley) at a dilution of 1:5,000 and monoclonal mouse anti-P60 antibody (Adipogen) at a dilution of 1:2,000. Goat anti-rabbit (Invitrogen) and goat anti-mouse (Li-Cor Biosciences) antibodies were used to detect the primary antibodies, each at a dilution of 1:5,000. Immunoblots were imaged on a Li-Cor Odyssey Fc system and were analyzed using Image Studio software to calculate band densitometry. All immunoblots were performed in biological triplicates.

Bacterial two-hybrid broth quantification. *E. coli* BTH101 strains, each containing one pUT18x vector (carbenicillin resistance) and one pKT25x vector (kanamycin resistance), were grown overnight at 37°C in LB broth containing kanamycin and carbenicillin. Cultures were permeabilized by combining 800 µl Z-Buffer, 20 µl 0.1% SDS, 40 µl chloroform, and 200 µl overnight culture. The assay was performed in a 96-well plate, and each strain was assayed in technical triplicates. Each well contained 150 µl Z-Buffer, 50-µl permeabilized culture solution, and 40 µl 0.4% *o*-nitrophenyl- β -D-galactopyranoside (ONPG) to start the reaction. A_{420} and A_{550} values were collected every 2 minutes for 30 minutes at 28°C. A_{420} data were graphed to determine the linear portion of the reaction, from which the calculations were performed. Miller units were calculated with the following equation: $[(A_{420} - (1.75 \times A_{550})) / (t \times v \times A_{600})] \times$

1,000 where t equals time in minutes and v equals culture volume used in the assay in milliliters (44). All BACTH data represent three biological replicates.

Whole-cell proteomics sample preparation. Wild-type and $\Delta yjbH$ *L. monocytogenes* were grown overnight and then subcultured for 5 h shaking at 37°C in BHI broth containing streptomycin. Cultures were then centrifuged for 20 minutes at 4°C. Pellets were sonicated in lysis buffer (0.1 M ammonium bicarbonate, 8 M urea, and 0.1% [wt/vol] Rapigest detergent [Waters]) and centrifuged at maximum speed. Tris(2-carboxyethyl)phosphine hydrochloride (TCEP) was added to supernatant fractions to a final concentration of 5 mM. Samples were incubated at room temperature for 1 hour before adding iodoacetamide to 10 mM. Samples were then incubated in the dark at room temperature for 30 minutes before adding *N*-acetylcysteine to 15 mM. Samples were then digested with trypsin gold (Promega) overnight at 37°C by combining 200 μ g of each sample (determined by BCA assay) with trypsin in a 1:20 (wt/wt) (trypsin/protein) ratio. Following trypsinization, 2 M HCl was added dropwise to each sample until samples became acidic (pH 1 to 2), as monitored with pH paper. Detergent was removed by centrifugation at $10,000 \times g$ for 5 minutes, and the supernatant was transferred into new tubes. Acetonitrile (ACN) and trifluoroacetic acid (TFA) were added to 5% and 0.1% (vol/vol), respectively. Samples were processed through MacroSpin C₁₈ columns (30- to 300- μ g capacity; The Nest Group) as directed and washed with 5% ACN and 0.1% TFA. Samples were eluted with 80% ACN and 25 mM formic acid. Samples were then sent to the Northwestern University Proteomics Core for analysis by mass spectrometry. The sample preparation protocol is adapted from the Mougous Laboratory at the University of Washington Department of Microbiology (45).

LC-MS/MS analysis. Peptides were analyzed by LC-MS/MS using a Dionex UltiMate 3000 rapid separation nanoLC instrument and an Orbitrap Elite mass spectrometer (Thermo Fisher Scientific, Inc., San Jose, CA). Samples were loaded onto the trap column, which was 150 μ m by 3 cm, and in-house packed with 3- μ m ReproSil-Pur beads. The analytical column was a 75- μ m by 10.5-cm PicoChip column packed with 3- μ m ReproSil-Pur beads (New Objective, Inc., Woburn, MA). The flow rate was kept at 300 nL/min. Solvent A was 0.1% formic acid (FA) in water and solvent B was 0.1% FA in ACN. The peptide was separated on a 120-min analytical gradient from 5% ACN/0.1% FA to 40% ACN/0.1% FA. MS¹ scans were acquired from 400 to 2,000 m/z at a 60,000 resolving power and with the automatic gain control (AGC) set to 1×10^6 intensity. The 15 most abundant precursor ions in each MS¹ scan were selected for fragmentation by collision-induced dissociation (CID) at 35% normalized collision energy in the ion trap. Previously selected ions were dynamically excluded from reselection for 60 seconds.

Data analysis. Proteins were identified from the MS raw files using the Mascot search engine (Matrix Science, London, UK; version 2.5.1). MS/MS spectra were searched against the UniProt *Listeria monocytogenes* database. All searches included carbamidomethyl cysteine as a fixed modification and oxidized Met, deamidated Asn and Gln, and acetylated N-term as variable modifications. Three missed tryptic cleavages were allowed. The MS¹ precursor mass tolerance was set to 10 ppm and the MS² tolerance was set to 0.6 Da. The search result was visualized by Scaffold (version 4.8.3; Proteome Software, Inc., Portland, OR). A 1% false discovery rate cutoff was applied at the peptide level. Only proteins with a minimum of two unique peptides above the cutoff were considered for further study.

Quantitative RT-PCR of bacterial transcripts. Overnight cultures of wild-type and $\Delta yjbH$ *L. monocytogenes* were diluted 1:100 into 25 ml of BHI in a 250-ml flask and grown in BHI broth at 37°C shaking until cultures reached an optical density at 600 nm (OD₆₀₀) of 1.0. At this point, 5 ml of each culture was pipetted into 5 ml ice-cold MeOH, inverted to mix, and centrifuged at 4°C to pellet. All supernatant was removed, and pellets were frozen in liquid nitrogen before storing at -80°C overnight.

Frozen pellets were resuspended in 400 μ l AE buffer (50 mM sodium acetate [NaOAc; pH 5.2] and 10 mM EDTA, diethyl pyrocarbonate [DEPC] treated and autoclaved) and vortexed vigorously. Samples were kept on ice as much as possible during entire protocol. A total of 400 μ l of the resuspended pellet mixture was transferred to an RNase-free 1.5-ml tube on ice containing 50 μ l 10% SDS and 500 μ l 1:1 acidified phenol-chloroform (made fresh, with aqueous layer removed before addition of the pellet mixture). Samples were then lysed by bead beating and returned to ice. Lysed samples were applied to prespun 5Prime phase lock gel heavy tubes (Quantabio) and centrifuged at maximum speed for 5 minutes. The aqueous layer was pipetted into a new 1.5-ml tube containing 50 μ l 3 M NaOAc at pH 5.2 and 1 ml 100% ethanol (EtOH) and was vortexed to mix. Samples were centrifuged at 4°C for 30 minutes at maximum speed, at which point the EtOH was removed by aspiration. A total of 500 μ l 70% EtOH was added to each sample and vortexed to mix. After centrifuging at room temperature for 10 minutes at maximum speed, the EtOH was removed by aspiration and then by running samples in a speed vac. Samples were resuspended in 50 μ l water and reverse transcribed using an iScript cDNA synthesis kit (Bio-Rad). Quantitative RT-PCR was performed on cDNA with the iTaq universal SYBR green supermix (Bio-Rad).

SUPPLEMENTAL MATERIAL

Supplemental material is available online only.

SUPPLEMENTAL FILE 1, XLSX file, 0.1 MB.

SUPPLEMENTAL FILE 2, PDF file, 0.5 MB.

ACKNOWLEDGMENTS

We thank members of the Reniere Lab for critical reading of the manuscript. We also thank the laboratory of Joseph Mougous (UW) for their generous help in whole-cell

proteomics preparation. Proteomics services were performed by the Northwestern Proteomics Core Facility, which is generously supported by NCI CCSG P30 CA060553 awarded to the Robert H. Lurie Comprehensive Cancer Center and the National Resource for Translational and Developmental Proteomics, supported by P41 GM108569.

Research in the Reniere Lab is funded by the National Institutes of Health (RO1 AI132356). B.R.R. is funded by the National Institute of General Medical Sciences (PHS NRSA T32GM007270). Research reported in this publication used an Azure Sapphire bioimager that was supported by the Office of the Director, National Institutes of Health under award number S10OD026741.

The content is solely the responsibility of the authors and does not necessarily represent the official views of the National Institutes of Health.

REFERENCES

- Ruhland BR, Reniere ML. 2019. Sense and sensor ability: redox-responsive regulators in *Listeria monocytogenes*. *Curr Opin Microbiol* 47:20–25. <https://doi.org/10.1016/j.mib.2018.10.006>.
- Cain JA, Solis N, Cordwell SJ. 2014. Beyond gene expression: the impact of protein post-translational modifications in bacteria. *J Proteomics* 97:265–286. <https://doi.org/10.1016/j.jprot.2013.08.012>.
- Bednarska NG, Schymkowitz J, Rousseau F, Van Eldere J. 2013. Protein aggregation in bacteria: the thin boundary between functionality and toxicity. *Microbiology* 159:1795–1806. <https://doi.org/10.1099/mic.0.069575-0>.
- Kuhlmann NJ, Chien P. 2017. Selective adaptor dependent protein degradation in bacteria. *Curr Opin Microbiol* 36:118–127. <https://doi.org/10.1016/j.mib.2017.03.013>.
- Reniere ML. 2018. Reduce, induce, thrive: bacterial redox sensing during pathogenesis. *J Bacteriol* 200:903. <https://doi.org/10.1128/JB.00128-18>.
- Freitag NE, Port GC, Miner MD. 2009. *Listeria monocytogenes*—from saprophyte to intracellular pathogen. *Nat Rev Microbiol* 7:623–628. <https://doi.org/10.1038/nrmicro2171>.
- Schnupf P, Portnoy DA. 2007. Listeriolysin O: a phagosome-specific lysin. *Microbes Infect* 9:1176–1187. <https://doi.org/10.1016/j.micinf.2007.05.005>.
- Kocks C, Gouin E, Tabouret M, Berche P, Ohayon H, Cossart P. 1992. *L. monocytogenes*-induced actin assembly requires the *actA* gene product, a surface protein. *Cell* 68:521–531. [https://doi.org/10.1016/0092-8674\(92\)90188-1](https://doi.org/10.1016/0092-8674(92)90188-1).
- Tilney LG, Portnoy DA. 1989. Actin filaments and the growth, movement, and spread of the intracellular bacterial parasite, *Listeria monocytogenes*. *J Cell Biol* 109:1597–1608. <https://doi.org/10.1083/jcb.109.4.1597>.
- Zemansky J, Kline BC, Woodward JJ, Leber JH, Marquis H, Portnoy DA. 2009. Development of a mariner-based transposon and identification of *Listeria monocytogenes* determinants, including the peptidyl-prolyl isomerase PrsA2, that contribute to its hemolytic phenotype. *J Bacteriol* 191:3950–3964. <https://doi.org/10.1128/JB.00016-09>.
- Reniere ML, Whiteley AT, Portnoy DA. 2016. An *in vivo* selection identifies *Listeria monocytogenes* genes required to sense the intracellular environment and activate virulence factor expression. *PLoS Pathog* 12:e1005741. <https://doi.org/10.1371/journal.ppat.1005741>.
- Rogstam A, Larsson JT, Kjelgaard P, Wachenfeldt von C. 2007. Mechanisms of adaptation to nitrosative stress in *Bacillus subtilis*. *J Bacteriol* 189:3063–3071. <https://doi.org/10.1128/JB.01782-06>.
- Göhring N, Fedtke I, Xia G, Jorge AM, Pinho MG, Bertsche U, Peschel A. 2011. New role of the disulfide stress effector YjbH in β -lactam susceptibility of *Staphylococcus aureus*. *Antimicrob Agents Chemother* 55:5452–5458. <https://doi.org/10.1128/AAC.00286-11>.
- Larsson JT, Rogstam A, Wachenfeldt von C. 2007. YjbH is a novel negative effector of the disulphide stress regulator, Spx, in *Bacillus subtilis*. *Mol Microbiol* 66:669–684. <https://doi.org/10.1111/j.1365-2958.2007.05949.x>.
- Chan CM, Garg S, Lin AA, Zuber P. 2012. *Geobacillus thermodenitrificans* YjbH recognizes the C-terminal end of *Bacillus subtilis* Spx to accelerate Spx proteolysis by ClpXP. *Microbiol* 158:1268–1278. <https://doi.org/10.1099/mic.0.057661-0>.
- Garg SK, Kommineni S, Henslee L, Zhang Y, Zuber P. 2009. The YjbH protein of *Bacillus subtilis* enhances ClpXP-catalyzed proteolysis of Spx. *J Bacteriol* 191:1268–1277. <https://doi.org/10.1128/JB.01289-08>.
- Engman J, Wachenfeldt von C. 2015. Regulated protein aggregation: a mechanism to control the activity of the ClpXP adaptor protein YjbH. *Mol Microbiol* 95:51–63. <https://doi.org/10.1111/mmi.12842>.
- Chan CM, Hahn E, Zuber P. 2014. Adaptor bypass mutations of *Bacillus subtilis* spx suggest a mechanism for YjbH-enhanced proteolysis of the regulator Spx by ClpXP. *Mol Microbiol* 93:426–438. <https://doi.org/10.1111/mmi.12671>.
- Zuber P. 2004. Spx-RNA polymerase interaction and global transcriptional control during oxidative stress. *J Bacteriol* 186:1911–1918. <https://doi.org/10.1128/JB.186.7.1911-1918.2004>.
- Newberry KJ, Nakano S, Zuber P, Brennan RG. 2005. Crystal structure of the *Bacillus subtilis* anti-alpha, global transcriptional regulator, Spx, in complex with the alpha C-terminal domain of RNA polymerase. *Proc Natl Acad Sci U S A* 102:15839–15844. <https://doi.org/10.1073/pnas.0506592102>.
- Rochat T, Nicolas P, Delumeau O, Rabatinová A, Korelusová J, Leduc A, Bessières P, Dervyn E, Krásny L, Noiro P. 2012. Genome-wide identification of genes directly regulated by the pleiotropic transcription factor Spx in *Bacillus subtilis*. *Nucleic Acids Res* 40:9571–9583. <https://doi.org/10.1093/nar/gks755>.
- Nakano S, Küster-Schöck E, Grossman AD, Zuber P. 2003. Spx-dependent global transcriptional control is induced by thiol-specific oxidative stress in *Bacillus subtilis*. *Proc Natl Acad Sci U S A* 100:13603–13608. <https://doi.org/10.1073/pnas.2235180100>.
- Kommineni S, Garg SK, Chan CM, Zuber P. 2011. YjbH-enhanced proteolysis of Spx by ClpXP in *Bacillus subtilis* is inhibited by the small protein YirB (YuzO). *J Bacteriol* 193:2133–2140. <https://doi.org/10.1128/JB.01350-10>.
- Awad W, Al-Eryani Y, Ekström S, Logan DT, Wachenfeldt von C. 2019. Structural basis for YjbH adaptor-mediated recognition of transcription factor Spx. *Structure* 27:923–936. <https://doi.org/10.1016/j.str.2019.03.009>.
- Arnér ES, Holmgren A. 2000. Physiological functions of thioredoxin and thioredoxin reductase. *Eur J Biochem* 267:6102–6109. <https://doi.org/10.1046/j.1432-1327.2000.01701.x>.
- Lu J, Holmgren A. 2014. The thioredoxin antioxidant system. *Free Radic Biol Med* 66:75–87. <https://doi.org/10.1016/j.freeradbiomed.2013.07.036>.
- Engman J, Rogstam A, Frees D, Ingmer H, von Wachenfeldt C. 2012. The YjbH adaptor protein enhances proteolysis of the transcriptional regulator Spx in *Staphylococcus aureus*. *J Bacteriol* 194:1186–1194. <https://doi.org/10.1128/JB.06414-11>.
- Wurtzel O, Sesto N, Mellin JR, Karunker I, Edelheit S, Bécavin C, Archambaud C, Cossart P, Sorek R. 2012. Comparative transcriptomics of pathogenic and non-pathogenic *Listeria* species. *Mol Syst Biol* 8:583. <https://doi.org/10.1038/msb.2012.11>.
- Sun AN, Camilli A, Portnoy DA. 1990. Isolation of *Listeria monocytogenes* small-plaque mutants defective for intracellular growth and cell-to-cell spread. *Infect Immun* 58:3770–3778. <https://doi.org/10.1128/IAI.58.11.3770-3778.1990>.
- Karimova G, Pidoux J, Ullmann A, Ladant D. 1998. A bacterial two-hybrid system based on a reconstituted signal transduction pathway. *Proc Natl Acad Sci U S A* 95:5752–5756. <https://doi.org/10.1073/pnas.95.10.5752>.

31. Battesti A, Bouveret E. 2012. The bacterial two-hybrid system based on adenylate cyclase reconstitution in *Escherichia coli*. *Methods* 58:325–334. <https://doi.org/10.1016/j.ymeth.2012.07.018>.
32. Whiteley AT, Ruhland BR, Edrozo MB, Reniere ML. 2017. A redox-responsive transcription factor is critical for pathogenesis and aerobic growth of *Listeria monocytogenes*. *Infect Immun* 85:e00978-16. <https://doi.org/10.1128/IAI.00978-16>.
33. Nakano MM, Nakano S, Zuber P. 2002. Spx (Yjbd), a negative effector of competence in *Bacillus subtilis*, enhances ClpC-MecA-ComK interaction. *Mol Microbiol* 44:1341–1349. <https://doi.org/10.1046/j.1365-2958.2002.02963.x>.
34. Nakano S, Zheng G, Nakano MM, Zuber P. 2002. Multiple pathways of Spx (Yjbd) proteolysis in *Bacillus subtilis*. *J Bacteriol* 184:3664–3670. <https://doi.org/10.1128/JB.184.13.3664-3670.2002>.
35. Austin CM, Garabaglu S, Krute CN, Ridder MJ, Seawell NA, Markiewicz MA, Boyd JM, Bose JL. 2019. Contribution of YjbH to virulence factor expression and host colonization in *Staphylococcus aureus*. *Infect Immun* 87:3012. <https://doi.org/10.1128/IAI.00155-19>.
36. Portman JL, Huang Q, Reniere ML, Iavarone AT, Portnoy DA. 2017. Activity of the pore-forming virulence factor listeriolysin O is reversibly inhibited by naturally occurring S-glutathionylation. *Infect Immun* 85:e00959-16. <https://doi.org/10.1128/IAI.00959-16>.
37. Nguyen BN, Peterson BN, Portnoy DA. 2019. Listeriolysin O: a phagosome-specific cytolysin revisited. *Cell Microbiol* 21:e12988. <https://doi.org/10.1111/cmi.12988>.
38. Bishop DK, Hinrichs DJ. 1987. Adoptive transfer of immunity to *Listeria monocytogenes*. The influence of *in vitro* stimulation on lymphocyte subset requirements. *J Immunol* 139:2005–2009.
39. Bécavin C, Bouchier C, Lechat P, Archambaud C, Creno S, Gouin E, Wu Z, Kühbacher A, Brisse S, Pucciarelli MG, García-del Portillo F, Hain T, Portnoy DA, Chakraborty T, Lecuit M, Pizarro-Cerdá J, Moszer I, Bierne H, Cossart P. 2014. Comparison of widely used *Listeria monocytogenes* strains EGD, 10403S, and EGD-e highlights genomic variations underlying differences in pathogenicity. *mBio* 5:e00969-14. <https://doi.org/10.1128/mBio.00969-14>.
40. Lauer P, Chow MYN, Loessner MJ, Portnoy DA, Calendar R. 2002. Construction, characterization, and use of two *Listeria monocytogenes* site-specific phage integration vectors. *J Bacteriol* 184:4177–4186. <https://doi.org/10.1128/JB.184.15.4177-4186.2002>.
41. Hodgson DA. 2000. Generalized transduction of serotype 1/2 and serotype 4b strains of *Listeria monocytogenes*. *Mol Microbiol* 35:312–323. <https://doi.org/10.1046/j.1365-2958.2000.01643.x>.
42. Whiteley AT, Garelis NE, Peterson BN, Choi PH, Tong L, Woodward JJ, Portnoy DA. 2017. c-di-AMP modulates *Listeria monocytogenes* central metabolism to regulate growth, antibiotic resistance and osmoregulation. *Mol Microbiol* 104:212–233. <https://doi.org/10.1111/mmi.13622>.
43. Schneider CA, Rasband WS, Eliceiri KW. 2012. NIH Image to ImageJ: 25 years of image analysis. *Nat Methods* 9:671–675. <https://doi.org/10.1038/nmeth.2089>.
44. Miller JH. 1972. Experiments in molecular genetics. Cold Spring Harbor Laboratory, Cold Spring Harbor, NY.
45. Ting S-Y, Bosch DE, Mangiameli SM, Radey MC, Huang S, Park Y-J, Kelly KA, Filip SK, Goo YA, Eng JK, Allaire M, Veessler D, Wiggins PA, Peterson SB, Mougous JD. 2018. Bifunctional immunity proteins protect bacteria against FtsZ-targeting ADP-ribosylating toxins. *Cell* 175:1380–1392. <https://doi.org/10.1016/j.cell.2018.09.037>.
46. Michna RH, Zhu B, Mäder U, Stülke J. 2016. SubtiWiki 2.0—an integrated database for the model organism *Bacillus subtilis*. *Nucleic Acids Res* 44:D654–D662. <https://doi.org/10.1093/nar/gkv1006>.
47. Mäder U, Nicolas P, Depke M, Pané-Farré J, Debarbouille M, van der Kooi-Pol MM, Guérin C, Dérozier S, Hiron A, Jarmer H, Leduc A, Michalik S, Reilman E, Schaffer M, Schmidt F, Bessières P, Noirot P, Hecker M, Msadek T, Völker U, van Dijk JM. 2016. *Staphylococcus aureus* transcriptome architecture: from laboratory to infection-mimicking conditions. *PLoS Genet* 12:e1005962. <https://doi.org/10.1371/journal.pgen.1005962>.